ORIGINAL ARTICLE

Cancer Science WILEY

PD-L1+ dendritic cells in the tumor microenvironment correlate with good prognosis and CD8+ T cell infiltration in colon cancer

Timothy J. Miller[1,2] | Chidozie C. Anyaegbu[1,2,3] | Tracey F. Lee-Pullen[1,2] |
Lisa J. Spalding[4] | Cameron F. Platell[1,2] | Melanie J. McCoy[1,2]

[1]Colorectal Research Unit, St. John of God Subiaco Hospital, Subiaco, WA, Australia

[2]Medical School, University of Western Australia, Crawley, WA, Australia

[3]Faculty of Health Sciences, Curtin Health Innovation Research Institute, Curtin University, Bentley, WA, Australia

[4]Harry Perkins Institute of Medical Research, Murdoch, WA, Australia

Correspondence
Timothy J. Miller, Medical School, University of Western Australia, Mail Bag 507, 35 Stirling Highway, Crawley, WA 6009, Australia.
Email: timothy.miller@uwa.edu.au

Funding information
This work was supported by the Cancer Council of Western Australia and the Tonkinson Colorectal Cancer Research Fund. The fluorescence scanning system was purchased for the Telethon Kids Institute with funding from Bright Blue, The Police Commissioner's Fund for Sick Kids. Purchase of the StrataQuest image analysis software was funded by the Tonkinson Colorectal Cancer Research Fund and the St John of God Foundation.

Abstract

Background: The prognostic value of tumor-associated dendritic cells (DC) in colon cancer remains poorly understood. This may be in part due to the interchangeable expression of immunostimulatory and immunoinhibitory molecules on DC. Here we investigated the prognostic impact of CD11c^{+} DC co–expressing the immunoinhibitory molecule PD-L1 and their spatial relationship with CD8^{+} T-cells in patients treated for stage III colon cancer.

Methods: Tissue microarrays containing representative cores of central tumor, leading edge, and adjacent normal tissue from 221 patients with stage III colon cancer were immunostained for CD8, CD11c, PD-L1, and cytokeratin using immunofluorescent probes. Cells were quantified using StrataQuest digital image analysis software, with intratumoral and stromal regions analyzed separately. Kaplan-Meier estimates and Cox regression were used to assess survival.

Results: Intratumoral CD8^{+} cell density (HR = .52, 95% confidence interval [CI] .33-.83, $P = .007$), stromal CD11c^{+} cell density (HR = .52, 95% CI .33-.83, $P = .006$), intratumoral CD11c^{+}PD-L1^{+} cell density (HR = .57, 95% CI .35-.92, $P = .021$), and stromal CD11c^{+}PD-L1^{+} cell density (HR = .48, 95% CI .30-.77, $P = .003$) on leading-edge cores were all significantly associated with good survival. CD8^{+} cell density was positively correlated with both CD11c^{+} cell density and CD11c^{+}PD-L1^{+} cell density in tumor epithelium and stromal compartments.

Conclusion: Here we showed that PD-L1-expressing DC in the tumor microenvironment are associated with improved survival in stage III colon cancer and likely reflect an immunologically "hot" tumor microenvironment. Further investigation into the expression of immunomodulatory molecules by tumor-associated DC may help to further elucidate their prognostic value.

KEYWORDS
CD8, colon cancer, dendritic cells, PD-L1, T cells

Timothy Miller and Chidozie Anyaegbu contributed equally to this work.

1 | INTRODUCTION

Despite advances in diagnosis and treatment, colorectal cancer (CRC) remains the second leading cause of cancer-related death worldwide.[1] Surgical resection with postoperative adjuvant chemotherapy is the standard-of-care for patients with stage III colon cancer; that is, cancer that has spread to the lymph nodes but has not yet metastasized to distant sites. Almost 30% of patients with stage III CRC die within 5 years of diagnosis,[2] highlighting a requirement for novel prognostic markers to identify patients who may benefit from more aggressive chemotherapy regimens.

The immune system plays an important role in cancer control and treatment response and it is increasingly recognized that key immune cell subtypes within the tumor microenvironment of CRC have prognostic potential. T-cell infiltration may even have greater prognostic value than TNM staging for patients with stage I-III colorectal cancer.[3-6] However, multiple mechanisms exist by which tumor cells may escape CD8^{+} T-cell-mediated destruction. One such mechanism is the hijacking of intrinsic immune checkpoint mechanisms, notably the programmed death receptor-1 (PD-1) signaling pathway. PD-ligand-1 (PD-L1) and, to a lesser extent, PD-ligand-2 (PD-L2) can be expressed on tumor, immune, endothelial, and muscle cells.[7-10] Binding of PD-L1/PD-L2 to PD-1, expressed by activated lymphocytes, can attenuate adaptive anti–tumor immune responses.[10] PD-L1 expression in tumor specimens is often used to predict response to PD-1/PD-L1 blockade therapy and in many cases, treatment is contingent upon demonstration of tumor-associated PD-L1 expression above a defined threshold using an approved companion diagnostic test.[11,12]

In colorectal cancer, tumor-associated PD-L1 expression has been associated with both good and poor clinical outcomes.[13,14] Recent evidence indicates that while PD-L1 expression by tumor cells is commonly associated with poor outcome or is not prognostic,[7,15-18] lymphocytic expression is associated with good clinical outcome.[7,15,16,18] This may reflect the different underlying mechanisms of PD-L1 expression by tumor cells and lymphocytes. Lymphocytes upregulate PD-L1 expression in response to adaptive immune responses, so higher PD-L1 expression may be reflective of higher levels of immune cell infiltration.[7,9,10] Whereas, in addition to cytokine-induced expression, underlying genetic aberrations have been demonstrated to amplify the PD-L1 gene in tumor cells, leading to constitutive expression of PD-L1 and, therefore, an association with poor survival outcomes.[9,19] While tumor PD-L1 expression has been shown to play a role in inhibiting T-cell responses,[20] recent studies suggest that dendritic cells (DC) are also a source of PD-L1 in the tumor microenvironment, a critical finding given their specialized ability to regulate T cell responses.[20-22]

Dendritic cells play a central role in the adaptive anti–tumor immune response. They act as sentinels, detect tumor antigens, present them to CD8^{+} T-cells, and supply necessary signals for both activation and suppression of CD8^{+} T-cells.[23,24] Studies investigating the clinical value of tumor-associated DC in CRC have found associations with both good[25-27] and poor[28] prognosis.

These conflicting reports may relate to the dual potential of DC to alternately promote and suppress immune responses, functions that are dependent on the DC subtype and/or the expression of activating or suppressive markers, such as PD-L1. This indicates that the functional status of DC may be of more relevance than their presence within tissue alone. PD-L1 expression by DC is known to influence CD8^{+} T cell priming and effector function,[20] and studies in CRC and other cancers have found CD11c^{+}PD-L1^{+} DC to be better predictors of response to anti–PD-L1 immunotherapy than PD-L1^{+} tumor cells.[21,28] Several studies have suggested that PD-L1 expression on myeloid antigen-presenting cells, not on tumor cells, may be the primary target of PD-1/PD-L1 blockade therapy.[22,29,30]

However, the prognostic value of DC PD-L1 expression in CRC has not been investigated. The difficulty in characterizing DC phenotypes within tissue samples may also explain the conflicting data relating to tumor-associated DC and prognosis.[23] Several different markers have been used to identify DC,[31] including CD11c, which is predominantly expressed by conventional DC, the subset of DC that specialize in driving CD8^{+} and CD4^{+} T cell-mediated anti–tumor immunity.[23] In addition, the proximity of DC to CD8^{+} T-cells could potentially impact their prognostic value, as this would influence the likelihood of a DC making the required stable interaction for modulation of T-cell function.[24]

In this study we used a 5-color multiplex immunofluorescence (IF) staining panel in conjunction with semi–automated tissue cytometry software to investigate the prognostic value of PD-L1-expressing DC in colon cancer. Using archival tumor specimens from a retrospective cohort of 221 patients with stage III colon cancer, we evaluated the relationship between cell subset density and patient survival for CD11c^{+} DC, CD11c^{+}PD-L1^{+} DC, and CD8^{+} T cells in the tumor microenvironment. Spatial relationships between CD11c^{+} or CD11c^{+}PD-L1^{+} DC and CD8^{+} T cells were also assessed. We hypothesized that a higher density of CD11c^{+}PD-L1^{+} DC would be associated with poor prognosis and their proximity to CD8^{+} T cells in the tumor microenvironment would also be associated with poor prognosis.

2 | MATERIALS AND METHODS

2.1 | Patient cohort

A cohort of 246 patients who underwent curative resection for colon cancer between 2000 and 2010 at various hospitals in Perth, Western Australia was retrospectively identified from hospital records and research databases. Inclusion criteria included diagnosis of stage III primary cancer at pathological review and at least one tumor specimen available for analysis. Exclusion criteria included a diagnosis of any stage other than stage III disease at pathological review, secondary cancer, or the absence of a tumor specimen available for analysis. Of the 246 patients, 118 were treated at St John of God (SJG) Subiaco Hospital, 95 at Royal Perth Hospital (RPH), and

33 at Sir Charles Gairdner Hospital (SCGH). The majority (77.8%) of patients received 5-fluorouracil-based adjuvant chemotherapy.

2.2 | Ethics

The use of tissue samples and clinicopathological data was approved by the SJG Health Care Human Research Ethics Committees (HREC) (ref. 1324) and the RPH HREC (ref. RGS01985). Recognition of approval was provided by the University of Western Australia and SCGH HREC. Patients treated at SJG Subiaco Hospital gave their written informed consent for use of their biological samples and health information to be used for research purposes. Use of biological samples and health information for patients treated at RPH and SCGH was approved under a waiver of consent. This study was performed in accordance with the Declaration of Helsinki.

2.3 | Tissue microarray construction

H&E-stained sections from each resection sample were reviewed by a pathologist and areas of interest were identified. Central tumor regions were selected from the geometric center of the tumor, avoiding areas of necrosis. Leading-edge regions were identified from the deep margin, targeting areas with evidence of tumor budding or other stromal interaction. Normal epithelium was selected from the longitudinal margins of the specimen (Figure S1). Tissue microarrays (TMA) containing 1-mm representative cores taken from the areas of interest were constructed from formalin-fixed paraffin embedded specimens using an MTA-1 Manual Tissue Arrayer (Beecher Instruments). For each case, two cores were taken from the central tumor; one core was taken from the leading edge and one core was taken from normal epithelium.

2.4 | Multiplex immunofluorescent staining

Multiplex immunofluorescent staining (IF) and image analysis was optimized and performed as previously described.[32] Sections 4-μm thick were cut from the TMA blocks and mounted on positively charged slides. Sections were dewaxed and rehydrated in a graded xylene and ethanol series before microwave treatment (MWT) in a 1100 W microwave (LG). MWT involved preheating Tris-EDTA (pH 9.0) solution in a microwave pressure cooker (Nordic Ware) for 8 minutes at 70% power. Slides were then placed in the preheated solution and heated for 2 minutes at 70% power before being removed from the microwave and allowed to cool to room temperature (RT). After MWT, endogenous peroxidase activity and non–specific IgG interactions were blocked using Peroxidazed 1 for 5 minutes and Background Sniper for 15 minutes at RT, respectively (Biocare Medical). Slides were incubated for 1 hour at RT for all primary antibodies, 30 minutes at RT for secondary reagents, and 10 minutes at

RT for tyramide signal amplification reagents (TSA) reagents, when used. TSA was used to amplify fluorescent signals and to allow stripping of antibody probes for subsequent application of antibodies raised in the same species.

The first cycle of staining utilized the rabbit anti–PD-L1 monoclonal antibody (1:500; 1.75 μg/mL, clone: E1L3N, Cell Signaling), Rabbit MACH-2 HRP Polymer (Biocare Medical), and TSA-Cy5 conjugate (1:50, Perkin-Elmer) before repeating MWT. Sections were then incubated with mouse monoclonal anti–CD8 antibody (1:8000; 19.63 ng/mL, clone: C8/144B, DAKO), Mouse MACH-2 HRP solution (Biocare Medical), and TSA-FITC conjugate (1:50, Perkin-Elmer) before repeating MWT again. An antibody cocktail that included a rabbit monoclonal anti–CD11c antibody (1:100; 1.03 μg/mL, clone: EP1347Y, Abcam) and a mouse anti–Cytokeratin antibody (1:50; 3.5 μg/mL, clones: AE1/AE3, DAKO) was then used. Sections were incubated with a secondary antibody cocktail that included an AF594-conjugated goat monoclonal anti–rabbit IgG antibody (1:50; 30 μg/mL, Jackson Immunoresearch) and an AF555-conjugated goat monoclonal anti–mouse IgG antibody (1:250; 8 μg/mL, Abcam). Nuclear staining was performed using DAPI for 5 minutes at RT (1:500; 10 μg/mL, Sigma-Aldrich). Slides were mounted using Prolong Diamond Antifade mounting media (Molecular Probes). Positive and negative control sections (stained with the full antibody panel and isotype antibodies at matched concentrations, respectively) and single-stain controls were included alongside the test TMA sections. Sections were stored at 4°C until image acquisition.

2.5 | Image acquisition

Images were acquired using a Pannoramic MIDI II fluorescence scanning system (3D Histech) equipped with an LED Spectra 6 light engine (Lumencor, Beaverton) and a pco.edge sCMOS camera (PCO). All slides were scanned using a 20×/NA 0.8 objective (Carl Zeiss), and camera settings were kept constant for all scans. Figure images were prepared using CaseViewer (3D Histech), Photoshop (Adobe), and StrataQuest version 6.0 (TissueGnostics). Technical specifications, filter configurations, and imaging settings are provided in Tables S1 and S2.

2.6 | Image analysis

Digital image analysis was performed using StrataQuest version 6.0. Display levels were consistent between images (Table S2). Images of each TMA were digitally "segmented" to analyze each individual tissue core separately. Tissue was automatically detected by StrataQuest, and where needed manual modifications were made to remove necrotic tissue, poor staining, and debris (Figure S2). Individual cells were identified with a nuclear segmentation algorithm using DAPI staining, together with a cellular mask around each nucleus to quantitate surface marker expression for each cell (Figure S2). $CD8^+$, $CD11c^+$, $CD11c^+PD-L1^+$, and $CD11c^+PD-L1^-$ cells

TABLE 1 Patient characteristics

Variable	n = 221
Age, median (interquartile range)	68.0 (60.0, 76.0)
Sex, n (%)	
Female	104 (47.1)
Male	117 (52.9)
Adjuvant chemotherapy, n (%)	
No	47 (21.3)
Yes	172 (77.8)
Not reported	2 (.9)
Site, n (%)	
Proximal	99 (44.8)
Caecum	38 (17.2)
Ascending colon	33 (14.9)
Hepatic flexure	10 (4.5)
Transverse colon	18 (8.1)
Distal	118 (53.4)
Splenic flexure	9 (4.1)
Descending colon	10 (4.5)
Sigmoid colon	80 (36.2)
Rectosigmoid junction	19 (8.6)
Not reported	4 (1.8)
T Stage, n (%)	
T1	3 (1.4)
T2	22 (10.0)
T3	127 (57.5)
T4	64 (29.0)
Not reported	5 (2.3)
N Stage, n (%)	
N1	141 (63.8)
N2	76 (34.4)
Not reported	4 (1.8)
Number of metastatic nodes, median (interquartile range)	3 (1, 5)
Lymphovascular invasion, n (%)	
Absent	110 (49.8)
Present	104 (47.1)
Not reported	7 (3.2)
Extramural vascular invasion, n (%)	
Absent	148 (67.0)
Present	61 (27.6)
Not reported	12 (5.4)
Perineural invasion, n (%)	
Absent	174 (78.7)
Present	38 (17.2)
Not reported	9 (4.1)
Grade, n (%)	

(Continues)

TABLE 1 (Continued)

Variable	n = 221
Low or moderate grade	158 (71.5)
High grade	32 (14.5)
Not reported	31 (14.0)
5-year survival, n (%)	
Alive	141 (63.8)
Died	80 (36.2)
Follow-up time (months), median	143.7

were identified using hierarchical gating of scattergrams displaying the staining intensity for each marker. Cell densities within different tissue compartments (epithelium vs stroma) were calculated using epithelial and stromal tissue detection, based on cytokeratin staining, allowing determination of both intratumoral and stromal densities for each cell type of interest (Figure S3). The density of CD8$^+$ cells within 0-10 μm, 10-100 μm, or >100 μm from either CD11c$^+$ or CD11c$^+$PD-L1$^+$ was quantitated by creating a digital overlay for either CD11c or CD11c/PD-L1, performing a distance transform from these overlays, and then calculating CD8$^+$ cell density within each distance zone (Figure S3). Area measurements and counts of each cell type for all regions of interest were exported and cell densities calculated.

2.7 | Statistical analysis

Correlations between the density of different cell types were analyzed using linear regression. The mean density was used where more than one tumor core was available for analysis. Categorical variables (high and low density of each cell type) were created using the median value as the cut-off. Overall survival, defined as time from surgery until death from any cause, was the endpoint used for survival analyses. Patients surviving more than 10 years after surgery were censored at 120 months. Kaplan-Meier survival curves were compared using the log-rank test and hazard ratios (HR) were calculated using univariate Cox regression. All variables with a $P < .05$ were included in the multivariate model. Hierarchical backward selection was used to determine the final model with variables $P < .05$ remaining in the model at each step. All P-values of $<.05$ were deemed significant.

SAS version 9.4 and GraphPad Prism 8 were used for statistical analysis.

2.8 | Power calculation

Based on previous studies, we anticipated that those patients with high CD11c$^+$PD-L1$^+$ density would have a median survival time of 5.8 years. With an accrual time of 10 years and a follow-up time of 60 months, this study was powered at 96.1% to detect an HR of 2.0 at $\alpha = .05$.

3 | RESULTS

3.1 | Patient characteristics

Patients were included in the analysis if at least one central tumor core of sufficient tissue integrity and staining quality was available (221 out of 246 patients). A leading-edge core was also available for 143 of these patients and a normal tissue core for 134 patients. Out of the 221 patients, 77.8% (172/221) received adjuvant chemotherapy and 63.8% (141/221) were alive 5 years after surgery (Table 1). The median age at surgery was 68 years and most patients had either T3 (57.5%) or T4 (29.0%) tumors. Other prominent features included 63.8% (141/221) of patients with fewer than three metastatic lymph nodes, 67.0% (148/221) without extramural venous invasion (EMVI), and 71.5% (158/221) with low or moderate grade histology. Median follow-up time for the cohort was 143.7 months (Table 1).

3.2 | CD8, CD11c, and PD-L1 expression

CD8, CD11c, and PD-L1 expression was localized to the cell membranes (Figure 1). Cells positive for CD8, CD11c, or PD-L1 were predominantly located in the stroma. CD11c$^+$PD-L1$^+$ double-positive cells were identified in both epithelial and stromal compartments but were rare across the cohort (Table S3 and Figure 2). The correlation between CD8$^+$ cell density and all other markers was tested using linear regression. In both tumor epithelium and stromal compartments, CD8$^+$ cell density was positively correlated with CD11c$^+$

cell density (R^2 = 25.83%, P < .001 and, R^2 = 18.26%, P < .001, respectively) and CD11c$^+$PD-L1$^+$ cell density (R^2 = 29.14%, P < .001 and, R^2 = 19.31%, P < .001, respectively; Figure 3).

3.3 | Univariate survival analysis

All clinicopathological factors and IF markers were assessed for their prognostic value in univariate Cox regression models. Follow-up time was censored at 120 months for patients surviving beyond this time point. Clinicopathological variables found to be significant markers of poor prognosis included increasing age, higher N stage, number of metastatic lymph nodes, and EMVI. Low-grade morphology and adjuvant chemotherapy treatment were significant markers of good prognosis (Table 2).

Immunological markers significantly associated with (good) prognosis included high intratumoral CD8$^+$ cell density, stromal CD11c$^+$ cell density, intratumoral CD11c$^+$PD-L1$^+$ cell density, and stromal CD11c$^+$PD-L1$^+$ cell density on leading-edge cores (Table 2; Figure 4). CD11c$^+$PD-L1$^-$ cell density was not associated with survival (Table 2; Figure 4G-H). When analyzed as percentage of CD11c$^+$ cells expressing PD-L1, the results were of borderline significance (Figure S4). Because the cohort included patients with tumors of all T stages, a subgroup analysis was performed including only patients with T3-T4 tumors. Results were consistent with the whole cohort analysis (Table S4). The small number of patients with T1-T2 tumors precluded meaningful analysis of this subgroup, so it is unknown whether the results are generalizable to patients with tumors in

FIGURE 1 Five-color multiplex immunofluorescence staining panel. Representative images of human colon cancer tissue showing each individual channel and five-color overlay of all channels. Details of the antibodies and fluorophores used are provided in the methods. Inset images for CD11c, PD-L1, and overlay panels display higher magnification of double-positive CD11c$^+$PD-L1$^+$ cells (arrowheads). Scale bars 50 μm and 20 μm (inset images)
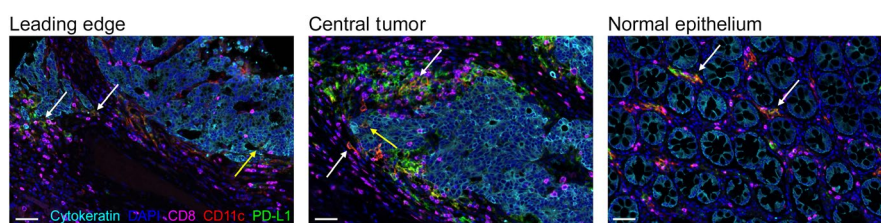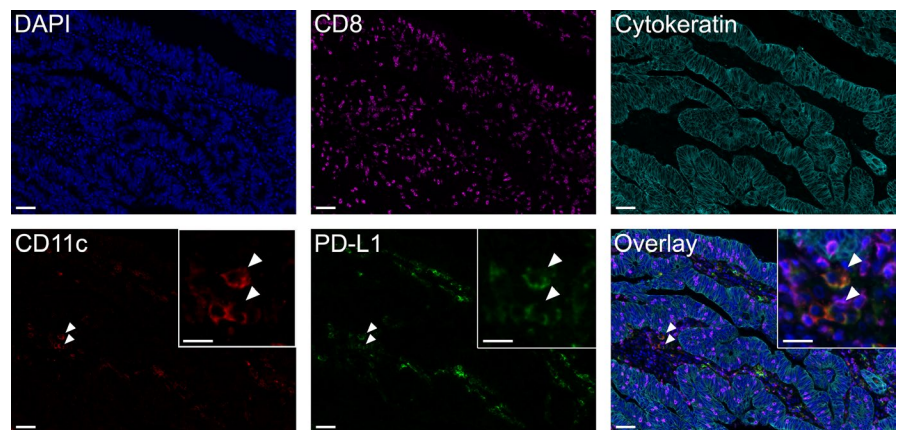
FIGURE 2 CD11c$^+$PD-L1$^+$ cells in the epithelium and stroma. Representative images of leading-edge tumor, central tumor, and normal colonic epithelium stained with cytokeratin (cyan), CD8 (magenta), CD11c (red), PD-L1 (green), and DAPI (blue). Arrows indicate double-positive CD11c$^+$PD-L1$^+$ cells in the stroma (white arrows) and epithelium (yellow arrows). Scale bars 50 μm
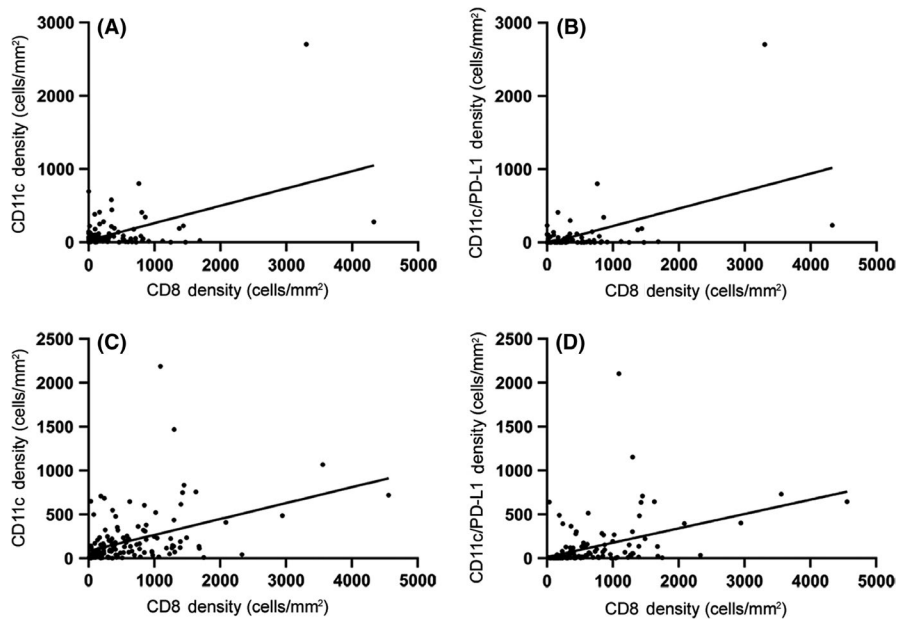
FIGURE 3 Correlation with CD8+ cell density. Linear regression of CD11c$^+$ cell density (A, C) and CD11c$^+$PD-L1$^+$ cell density (B, D) versus CD8$^+$ cell density in tumor epithelium (A, B) and stromal tissue (C, D). Each dot represents an individual tissue core

which invasion is limited to the submucosa/muscularis propria. High intratumoral CD8$^+$ cell density was associated with good prognosis in central tumor cores. High intra-epithelial CD8$^+$ cell density was also a poor prognostic marker in normal tissue (Table S5). Subsequent analyses focused on leading-edge cores only.

Spatial analysis was performed by calculating CD8$^+$ cell density and the proportion of total CD8$^+$ cells within 10 μm, within 100 μm, and over 100 μm from the closest CD11c$^+$ or CD11c$^+$PD-L1$^+$ cells. All statistical analyses for distance zones were adjusted for total CD11c$^+$ or CD11c$^+$PD-L1$^+$ cell density. Both CD8$^+$ cell density and the proportion of CD8$^+$ cells within each distance zone were assessed for prognostic significance. Neither was found to be associated with survival within any of the distance zones (Table S6).

3.4 | Multivariate survival analysis

Multivariate Cox regression was used to assess independent associations with prognosis. Backward selection was performed on all variables with $P < .05$ in the univariate Cox regression. Two models were tested, both of which included age at surgery, adjuvant chemotherapy, number of metastatic lymph nodes, EMVI, histological grade, and intratumoral CD8$^+$ cell density. To avoid mathematical coupling,[33] one of the multivariate models included stromal CD11c$^+$ cell density and the other intratumoral and stromal CD11c$^+$PD-L1$^+$ cell density (Table 3).

In model 1 (including CD11c$^+$ cell density), adjuvant chemotherapy, number of metastatic lymph nodes, EMVI, histological grade, intratumoral CD8$^+$ cell density, and stromal CD11c$^+$ cell density were independent prognostic factors for improved overall survival. In model 2 (including CD11c$^+$PD-L1$^+$ cell density), age at surgery, histological grade, and stromal CD11c$^+$PD-L1$^+$ cell density were independent prognostic factors for improved overall survival (Table 3).

4 | DISCUSSION

The phenotype and localization of various immune cell types in different areas of the tumor microenvironment are important histopathological features with prognostic value.[34] This study investigated PD-L1 expression on tumor-associated DC in relation to CD8$^+$ cell infiltration and clinical outcome in a cohort of patients with stage III colon cancer. We assessed the density of CD11c$^+$ DC and PD-L1-expressing CD11c$^+$ DC and their spatial interaction with CD8$^+$ cells in the tumor center, tumor leading edge, and normal uninvolved adjacent tissue. Our initial hypotheses were that high CD11c$^+$PD-L1$^+$ cell density would be associated with poor survival and that proximity of these cells to CD8$^+$ T-cells would also be associated with poor prognosis. In contrast to this, we found that high CD11c$^+$PD-L1$^+$ density in the epithelium and stroma at the tumor leading edge was associated with good prognosis and that the distance of these cells to CD8$^+$ T-cells was not prognostic. Our data indicate that the prognostic value of CD11c$^+$ cell density is driven by the CD11c$^+$PD-L1$^+$ cell population, as evidenced by the lack of association between CD11c$^+$PD-L1$^-$ cell density and survival. The results of this study also indicate that these associations were strongest in the stromal compartment, indicating that the interplay between these and other immune cell types in the tumor microenvironment has the greatest impact on survival.

Programmed death receptor-1 expression is induced by proinflammatory cytokines, including type I and type II interferons during an active immune response.[10] It is now widely accepted that high CD8$^+$ cell density is a good prognostic marker in colorectal cancer and indicates an "immunologically hot" tumor microenvironment.[3,35] Therefore, a likely explanation for the observed association between high CD11c$^+$PD-L1$^+$ density and improved survival is that the presence of PD-L1$^+$ DC in the local tumor environment is reflective of a preexisting anti–tumor response. In support of this, we found a strong positive correlation between CD8$^+$ cell density and

TABLE 2 Univariate Cox regression for clinicopathological and immune-related variables

Variable	Univariate		
	HR	95% CI	*P*
Age at surgery	1.03	1.01-1.05	<.001*
Sex			
Female	.76	.52-1.09	.137
Male	1.00		
Adjuvant chemotherapy			
Yes	.51	.35-.77	.001*
No	1.00		
Site			.382
Unknown	.31	.04-2.25	.248
Distal	.85	.59-1.22	.378
Proximal	1.00		
T Stage			.212
Unknown	.48	.12-1.99	.313
T1	.33	.05-2.37	.267
T2	.51	.25-1.05	.068
T3	.71	.48-1.05	.088
T4	1.00		
N Stage			
N1	.62	.43-.91	.013*
N2	1.00		
Number of metastatic nodes	1.04	1.01-1.07	.009*
Lymphovascular Invasion			.350
Not Reported	.78	.25-2.50	.677
Present	1.28	.88-1.84	.193
Absent	1.00		
Extramural venous invasion			.002*
Not reported	.82	.33-2.03	.665
Present	1.94	1.32-2.85	<.001*
Absent	1.00		
Perineural invasion			.276
Not reported	.62	.20-1.94	.408
Present	1.36	.86-2.14	.193
Absent	1.00		
Grade			<.001*
Not reported	.63	.35-1.15	.133
Low/moderate grade	.39	.25-.62	<.001*
High Grade	1.00		
CD8+ cell density - Leading Edge (high vs low)			
Tumor	.52	.33-.83	.007*
Stroma	.69	.43-1.09	.114
CD11c+ cell density - Leading Edge (high vs low)			

(Continues)

TABLE 2 (Continued)

Variable	Univariate		
	HR	95% CI	*P*
Tumor	.80	.51-1.27	.343
Stroma	.52	.33-.83	.006*
CD11c+PD-L1+ cell density - Leading Edge (high vs low)			
Tumor	.57	.35-.92	.021*
Stroma	.48	.30-.77	.003*
CD11c+PD-L1- cell density - Leading Edge (high vs low)			
Tumor	.88	.56-1.40	.595
Stroma	.84	.53-1.32	.438

*Significant values.

CD11c+PD-L1+ cell density (Figure 3). This is consistent with previous studies demonstrating an association between tumor-associated PD-L1 expression and increased lymphocytic infiltration in CRC and other cancers.[13,36-38] However, our multivariate analyses demonstrated that stromal CD11c+PD-L1+ density was independently prognostic, indicating that the association between the presence of this cell population and improved survival is not entirely due to the correlation with CD8+ T cell infiltration.

Although our results indicate that PD-L1 expressing CD11c+ DC are associated with good prognosis, it should be acknowledged that these cells could still be acting as negative regulators of a CD8+ T-cell-driven anti–tumor response. Studies investigating the role of PD-L1+ DC in PD-L1 blockade therapy have demonstrated that PD-L1 on DC prevents reactivation of exhausted, tumor-specific CD8+ T-cells.[30,39] Using tumor specimens from patients with lung cancer and an in vitro system using monocyte-derived DC, Mayoux et al showed that PD-L1 and CD80 on intratumoral DC bind in *cis*, preventing the costimulatory interaction between CD28 on T cells and CD80 and allowing PD-L1-PD-1-mediated cross-inhibition of CD28 signaling to keep T cells inactive.[30] In line with this mechanism, a high density of CD11c+PD-L1+ DC in biopsies of patients with CRC is predictive of response to PD-L1 blockade.[28] Together, these findings support a hypothetical model in which PD-L1 on DC keeps T-cells that were initially reactive to tumors (and therefore may have contributed to the good prognosis) unresponsive. Using a different in vitro system, Zhao et al also demonstrated that PD-L1 and CD80 form heterodimers on the surface of antigen-presenting cells (APC).[40] However, they found that this inhibited PD-1-PD-L1 and CD80-CTLA-4 interaction, without inhibiting CD80-CD28 binding, thus presenting a model whereby PD-L1 expression on APC can have an immunostimulatory effect. This may help to explain our finding that tumor-associated PD-L1+ DC are associated with good prognosis.

While these models describe the role of CD11c+PD-L1+ DC, they raise mechanistic questions about how CD11c+PD-L1+ DC sustain contact with T cells to maintain suppression, despite being
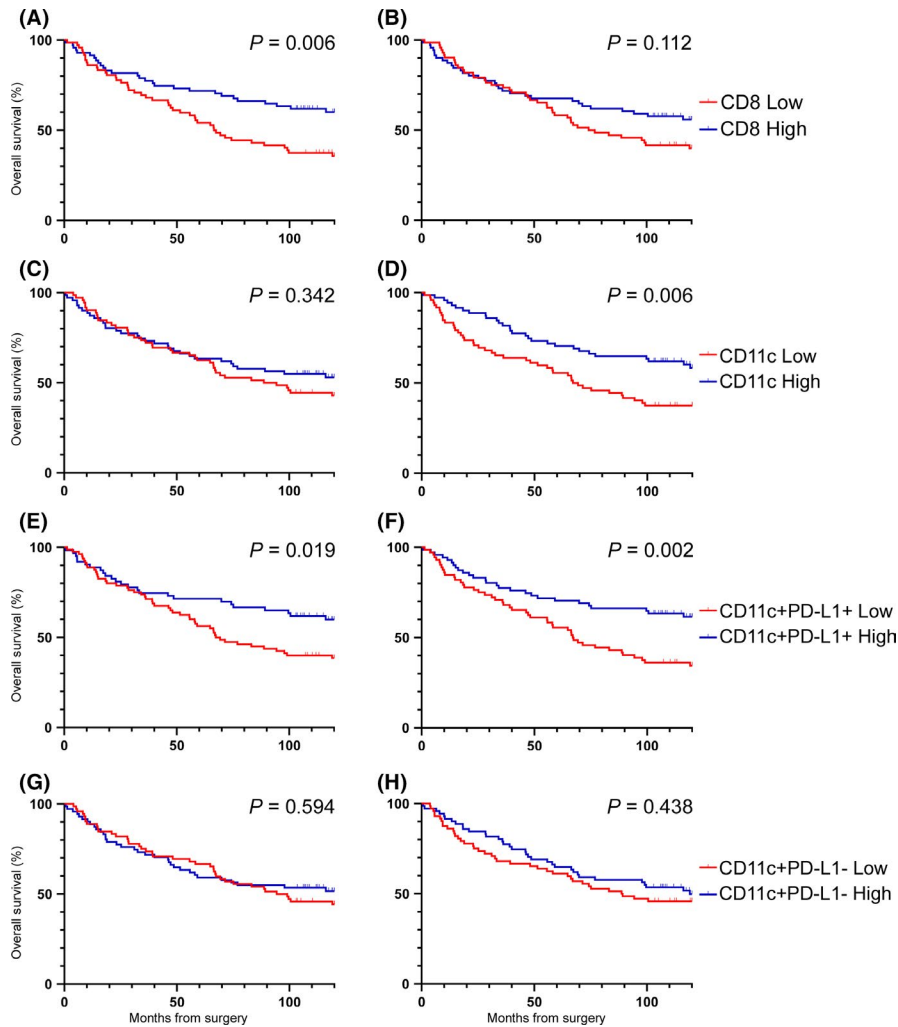
FIGURE 4 Overall survival by cell density. Survival curves for CD8^{+} (A-B), CD11c^{+} (C-D), CD11c^{+}PD-L1^{+} (E-F), and CD11c^{+}PD-L1^{−} (G-H) cell densities in tumor (A, C, E, G) and stromal (B, D, F, H) regions of leading-edge cores. Log-rank P-values are presented

a sparse population in the tumor microenvironment. We found a lack of association between the proximity of CD11c^{+}PD-L1^{+} cells to CD8^{+} cells and prognosis. This finding could, in part, relate to the limited number of patients with samples suitable for inclusion in this analysis, as leading-edge samples from just 44 patients contained both CD8^{+} cells and CD11c^{+}PD-L1^{+} cells, limiting the power of this analysis. Alternatively, it could suggest that tumor-associated CD11c^{+}PD-L1^{+} DC employ indirect mechanisms to regulate CD8^{+} T-cells, such as activating PD-1^{+} regulatory CD4^{+} T cells.[41] CD4^{+} T cells were not investigated in the current study due to limitations on multiplex panel size using the system available to us. However, CD4^{+} T cells also play an important role in anti−tumor immunity. CD4^{+} T cell infiltration correlates with PD-L1 expression in stage III colon tumors,[42] infiltrating CD4^{+} T cells express multiple checkpoint molecules, including PD-1,[43-45] and PD-L1 blockade induces expansion of CD4^{+} T cells co−expressing both inhibitory and activating checkpoint molecules.[43]

We also found that marker expression within leading-edge cores was more clinically significant than within central tumor cores. This may reflect the higher immune cell densities observed in leading-edge cores for all markers (data not shown). In addition, it has been consistently reported that immune cell density at the leading edge (or invasive margin) holds strong clinical significance.[3,4,46,47] This finding is, therefore, consistent with the literature.

One limitation of this study was the inability to accurately adjust for the effect of adjuvant chemotherapy on survival. This was due to incomplete data regarding details of the chemotherapy regimens administered, including drug combinations, dosages, and number of cycles administered, which is a common limitation of retrospective studies. Data regarding reasons for patients not receiving adjuvant chemotherapy were also limited. Where data were available, patients were judged to be too frail to undergo chemotherapy, with a small number refusing treatment for personal reasons. Follow-up studies could assess the prognostic effect of these markers in a cohort of patients with complete adjuvant treatment information or in patients that did not receive adjuvant treatment, such as patients with stage I and low-risk stage II CRC. It should also be acknowledged that the size of our patient cohort was relatively small, and our findings require validation in independent studies.

Another potential limitation was that identification of DC was based on expression of CD11c alone. While CD11c is recognized as a marker of conventional DC, it is important to note that CD11c can also be expressed by other cells of myeloid origin.[23] We were unable to include multiple DC markers due to the limitation on panel

TABLE 3 Multivariate Cox regression for variables significantly associated with survival in univariate analysis

Variable	Multivariate model 1			Multivariate model 2		
	HR	95% CI	P	HR	95% CI	P
Age at surgery			.120	1.03	1.01-1.05	.010*
Adjuvant chemotherapy						
Yes	.43	.25-.75	.003*			.267
No	1.00					
Number of metastatic nodes	1.04	1.01-1.08	.050[a],*			.110
Extramural venous invasion			.044*			.112
Not reported	1.75	.60-5.13	.308			
Present	1.89	1.13-3.14	.015*			
Absent	1.00					
Grade			.003*			<.001*
Not reported	.54	.24-1.20	.130	.36	.16-.78	.103
Low/moderate	.36	.20-.65	<.001*	.27	.15-.47	<.001*
High	1.00			1.00		
CD8+ cell density – Leading edge						
Tumor	.49	.29-.83	.008*			.059
Stroma						
CD11c+ cell density – Leading edge						
Tumor			–			
Stroma	.56	.34-.92	.023*			–
CD11c+PD-L1+ cell density – Leading edge						
Tumor			–			.785
Stroma			–	.46	.28-.75	.002*

[a]Actual value .0497.
*Significant values.

size. This precluded assessment of the prognostic contributions of CD11c+ conventional DC1 and DC2 subsets, which preferentially activate CD8+ T-cells and CD4+ T-cells (including CD4+ regulatory T-cells), respectively.[23] Inclusion of additional DC subset markers may allow more definitive identification of inhibitory and stimulatory DC subsets and investigation of their prognostic value.

We also acknowledge that PD-L1 staining pattern and intensity can vary depending on the antibody clone used.[48,49] We elected to use E1L3N in the current study as in our previous evaluation of four anti–PD-L1 clones.[50] We found that E1L3N produced the strongest and most complete membranous staining on FFPE colorectal cancer samples and was least affected by changes in antigen retrieval and signal detection methods. The membranous localization of PD-L1 staining we observed is consistent with the structural characterization of PD-L1 as a transmembrane glycoprotein.[51] Of note, Polioudaki et al recently suggested that conflicting reports of cytoplasmic[52] and nuclear[53] PD-L1 staining in FFPE colorectal tissues

may relate to "mis-localization" of PD-L1 from the cell membrane following tissue fixation.[54]

To our knowledge, this is the first study to demonstrate that PD-L1+ tumor-associated DC correlate with increased CD8+ T cell infiltration and are associated with improved survival in colon cancer. The presence of PD-L1+ DC in the local tumor environment may reflect an active CD8+ T-cell-driven anti–tumor immune response. Further studies assessing the prognostic value of tumor-associated DC subsets and their expression of immunoinhibitory or stimulatory markers are warranted to fully elucidate the prognostic value of tumor-associated DC in CRC.

with microtomy, and Dr Jeremy Parry of Western Diagnostics and Dr Kim Cheah of Dorevitch Pathology for reviewing cases and selecting regions of interest for TMA construction. We would also like to thank Dr Tim Threlfall of the Western Australian Cancer Registry, Cheryl Penter of St John of God Subiaco Hospital, and Prof Andrew Redfern of Harry Perkins Institute of Medical Research for assistance with data collection and access to patient samples. We thank our consumer representative Mr Terry Ianello for providing valuable input at the onset of this study.

CONFLICT OF INTEREST

ORCID
Timothy J. Miller https://orcid.org/0000-0002-0473-1869

REFERENCES

1. Bray F, Ferlay J, Soerjomataram I, Siegel RL, Torre LA, Jemal A. Global cancer statistics 2018: GLOBOCAN estimates of incidence and mortality worldwide for 36 cancers in 185 countries. *CA Cancer J Clin*. 2018;68:394-424.
2. Australian Institute of Health and Welfare. *Cancer data in Australia*. Canberra, ACT: Australian Institute of Health and Welfare; 2019.
3. Angell HK, Bruni D, Barrett JC, Herbst R, Galon J. The immunoscore: Colon cancer and beyond. *Clin Cancer Res*. 2020;26:332-339.
4. Galon J, Costes A, Sanchez-Cabo F, et al. Type, density, and location of immune cells within human colorectal tumors predict clinical outcome. *Science*. 2006;313:1960-1964.
5. Mlecnik B, Tosolini M, Kirilovsky A, et al. Histopathologic-based prognostic factors of colorectal cancers are associated with the state of the local immune reaction. *J Clin Oncol*. 2011;29:610-618.
6. Pagès F, Mlecnik B, Marliot F, et al. International validation of the consensus Immunoscore for the classification of colon cancer: a prognostic and accuracy study. *Lancet*. 2018;391:2128-2139.
7. Calik I, Calik M, Turken G, et al. Intratumoral cytotoxic T-lymphocyte density and PD-L1 expression are prognostic biomarkers for patients with colorectal cancer. *Medicina*. 2019;55:723.
8. Dong H, Zhu G, Tamada K, Chen L. B7–H1, a third member of the B7 family, co–stimulates T-cell proliferation and interleukin-10 secretion. *Nat Med*. 1999;5:1365-1369.
9. Ribas A, Hu-Lieskovan S. What does PD-L1 positive or negative mean? *J Exp Med*. 2016;213:2835-2840.
10. Boussiotis VA. Molecular and Biochemical Aspects of the PD-1 Checkpoint Pathway. *N Engl J Med*. 2016;375:1767-1778.
11. Davis AA, Patel VG. The role of PD-L1 expression as a predictive biomarker: an analysis of all US Food and Drug Administration (FDA) approvals of immune checkpoint inhibitors. *J Immunother Cancer*. 2019;7:278.
12. Sunshine J, Taube JM. PD-1/PD-L1 inhibitors. *Curr Opin Pharmacol*. 2015;23:32-38.
13. Droeser RA, Hirt C, Viehl CT, et al. Clinical impact of programmed cell death ligand 1 expression in colorectal cancer. *Eur J Cancer*. 2013;49:2233-2242.
14. Shi SJ, Wang LJ, Wang GD, et al. B7–H1 expression is associated with poor prognosis in colorectal carcinoma and regulates the proliferation and invasion of HCT116 colorectal cancer cells. *PLoS One*. 2013;8:e76012.
15. Berntsson J, Eberhard J, Nodin B, et al. Expression of programmed cell death protein 1 (PD-1) and its ligand PD-L1 in colorectal cancer: Relationship with sidedness and prognosis. *Oncoimmunology*. 2018;7:e1465165.

16. Lee KS, Kwak Y, Ahn S, et al. Prognostic implication of CD274 (PD-L1) protein expression in tumor-infiltrating immune cells for microsatellite unstable and stable colorectal cancer. *Cancer Immunol Immunother*. 2017;66:927-939.
17. Lee LH, Cavalcanti MS, Segal NH, et al. Patterns and prognostic relevance of PD-1 and PD-L1 expression in colorectal carcinoma. *Mod Pathol*. 2016;29:1433-1442.
18. Solomon B, Young RJ, Bressel M, et al. Prognostic Significance of PD-L1+ and CD8+ Immune Cells in HPV+ Oropharyngeal Squamous Cell Carcinoma. *Cancer Immunol Res*. 2018;6:295-304.
19. Chen S, Crabill GA, Pritchard TS, et al. Mechanisms regulating PD-L1 expression on tumor and immune cells. *J Immunother Cancer*. 2019;7:305.
20. Gibbons Johnson RM, Dong H. Functional expression of programmed death-ligand 1 (B7–H1) by immune cells and tumor cells. *Front Immunol*. 2017;8:961.
21. Lin H, Wei S, Hurt EM, et al. Host expression of PD-L1 determines efficacy of PD-L1 pathway blockade-mediated tumor regression. *J Clin Invest*. 2018;128:805-815.
22. Tang H, Liang Y, Anders RA, et al. PD-L1 on host cells is essential for PD-L1 blockade-mediated tumor regression. *J Clin Invest*. 2018;128:580-588.
23. Böttcher JP, Reis e Sousa C. The role of type 1 conventional dendritic cells in cancer immunity. *Trends in Cancer*. 2018;4:784-792.
24. Suzuki A, Masuda A, Nagata H, et al. Mature dendritic cells make clusters with T cells in the invasive margin of colorectal carcinoma. *J Pathol*. 2002;196:37-43.
25. Gulubova MV, Ananiev JR, Vlaykova TI, et al. Role of dendritic cells in progression and clinical outcome of colon cancer. *Int J Colorectal Dis*. 2012;27:159-169.
26. Kocian P, Sedivcova M, Drgac J, et al. Tumor-infiltrating lymphocytes and dendritic cells in human colorectal cancer: their relationship to KRAS mutational status and disease recurrence. *Hum Immunol*. 2011;72:1022-1028.
27. Michea P, Noel F, Zakine E, et al. Adjustment of dendritic cells to the breast-cancer microenvironment is subset specific. *Nat Immunol*. 2018;19:885-897.
28. Herbst RS, Soria JC, Kowanetz M, et al. Predictive correlates of response to the anti–PD-L1 antibody MPDL3280A in cancer patients. *Nature*. 2014;515:563-567.
29. Garris CS, Arlauckas SP, Kohler RH, et al. Successful anti–PD-1 cancer immunotherapy requires T cell-dendritic cell crosstalk involving the cytokines IFN-gamma and IL-12. *Immunity*. 2018; 49: 1148-1161.
30. Mayoux M, Roller A, Pulko V, et al. Dendritic cells dictate responses to PD-L1 blockade cancer immunotherapy. *Sci Transl Med*. 2020;12:eaav7431.
31. Hubert M, Gobbini E, Bendriss-Vermare N, Caux C, Valladeau-Guilemond J. Human Tumor-Infiltrating Dendritic Cells: From in Situ Visualization to High-Dimensional Analyses. *Cancers*. 2019;11:1082.
32. Anyaegbu CC, Lee-Pullen TF, Miller TJ, et al. Optimisation of multiplex immunofluorescence for a non-spectral fluorescence scanning system. *J Immunol Methods*. 2019;472:25-34.
33. Archie JPJ. Mathematic coupling of data: A common source of error. *Ann Surg*. 1981;193:296-303.
34. Fridman WH, Zitvogel L, Sautes-Fridman C, Kroemer G. The immune contexture in cancer prognosis and treatment. *Nat Rev Clin Oncol*. 2017;14:717-734.
35. Sharma P, Allison JP. The future of immune checkpoint therapy. *Science*. 2015;348:56-61.
36. Schalper KA, Velcheti V, Carvajal D, et al. In situ tumor PD-L1 mRNA expression is associated with increased TILs and better outcome in breast carcinomas. *Clin Cancer Res*. 2014;20:2773-2782.
37. Taube JM, Anders RA, Young GD, et al. Colocalization of inflammatory response with B7–H1 expression in human melanocytic lesions

supports an adaptive resistance mechanism of immune escape. *Sci Transl Med.* 2012;4:127ra37.

38. Webb JR, Milne K, Kroeger DR, Nelson BH. PD-L1 expression is associated with tumor-infiltrating T cells and favorable prognosis in high-grade serous ovarian cancer. *Gynecol Oncol.* 2016;141:293-302.

39. Kamphorst AO, Wieland A, Nasti T, et al. Rescue of exhausted CD8 T cells by PD-1-targeted therapies is CD28-dependent. *Science.* 2017;355:1423-1427.

40. Zhao Y, Lee CK, Lin C-H. PD-L1:CD80 Cis-Heterodimer Triggers the Co–stimulatory Receptor CD28 While Repressing the Inhibitory PD-1 and CTLA-4 Pathways. *Immunity.* 2019;51:1059-1073.

41. Francisco LM, Salinas VH, Brown KE, et al. PD-L1 regulates the development, maintenance, and function of induced regulatory T cells. *J Exp Med.* 2009;206:3015-3029.

42. Jung DH, Park HJ, Jang HH, et al. Clinical Impact of PD-L1 Expression for Survival in Curatively Resected Colon Cancer. *Cancer Invest.* 2020;38:406-414.

43. Beyrend G, van der Gracht E, Yilmaz A, et al. PD-L1 blockade engages tumor-infiltrating lymphocytes to co–express targetable activating and inhibitory receptors. *J Immunother Cancer.* 2019;7:217.

44. Di J, Liu M, Fan Y, et al. Phenotype molding of T cells in colorectal cancer by single-cell analysis. *Int J Cancer.* 2020;146:2281-2295.

45. Toor SM, Murshed K, Al-Dhaheri M, et al. Immune checkpoints in circulating and tumor-infiltrating CD4(+) T cell subsets in colorectal cancer patients. *Front Immunol.* 2019;10:2936.

46. Mlecnik B, Bindea G, Angell HK, et al. Integrative Analyses of Colorectal Cancer Show Immunoscore Is a Stronger Predictor of Patient Survival Than Microsatellite Instability. *Immunity.* 2016;44:698-711.

47. Vayrynen JP, Tuomisto A, Klintrup K, et al. Detailed analysis of inflammatory cell infiltration in colorectal cancer. *Br J Cancer.* 2013;109:1839-1847.

48. Hirsch FR, McElhinny A, Stanforth D, et al. PD-L1 Immunohistochemistry Assays for Lung Cancer: Results from Phase 1 of the Blueprint PD-L1 IHC Assay Comparison Project. *J Thorac Oncol.* 2017;12:208-222.

49. Udall M, Rizzo M, Kenny J, et al. PD-L1 diagnostic tests: a systematic literature review of scoring algorithms and test-validation metrics. *Diagn Pathol.* 2018;13:12.

50. Anyaegbu CC, Garrett K, Hemmings C, Lee-Pullen TF, McCoy MJ. Immunohistochemical detection of PD-L1 for research studies: which antibody and what protocol? *Pathology.* 2017;49:427-430.

51. Zak KM, Grudnik P, Magiera K, et al. Structural biology of the immune checkpoint receptor PD-1 and its ligands PD-L1/PD-L2. *Structure.* 2017;25:1163-1174.

52. Shan T, Chen S, Wu T, et al. PD-L1 expression in colon cancer and its relationship with clinical prognosis. *Int J Clin Exp Pathol.* 2019;12:1764-1769.

53. Satelli A, Batth IS, Brownlee Z, et al. Potential role of nuclear PD-L1 expression in cell-surface vimentin positive circulating tumor cells as a prognostic marker in cancer patients. *Sci Rep.* 2016;6:28910.

54. Polioudaki H, Chantziou A, Kalyvianaki K, et al. Nuclear localization of PD-L1: artifact or reality? *Cell Oncol (Dordr).* 2019;42:237-242.

SUPPORTING INFORMATION

Additional supporting information may be found online in the Supporting Information section.